Journal of the Geological Society, *London*, Vol. **166**, 2009, pp. 205–216. doi: 10.1144/0016-76492008-064.

Faulting and fluid flow through salt

IAN DAVISON

Earthmoves Ltd, Chartley, 38–42 Upper Park Road, Camberley GU15 2EF, UK

(e-mail: i.davison@earthmoves.co.uk)

Abstract: Halite and other evaporite rocks are often considered to be viscous materials that never deform by brittle faulting. However, fractures and faults are observed very locally in some salt domes and glaciers, and are indicated by data or shocks from seismically active areas. Rock mechanics experiments show that halite begins to deform by faulting once strain rates are large enough. However, it is very rare that such high strain rates occur in salt. Faulting in salt is most likely to occur where effective confining stress is significantly decreased by fluid overpressure, so that the salt fails at much lower differential stress. Several examples are presented of dilational veins oriented in several directions, which strongly indicate the presence of overpressured fluids during fracturing. Hydrocarbon maturation in shales deposited within the salt interval or metamorphic reactions of evaporite minerals often produce fluid overpressure. Mining-induced fractures in the Boulby Mine, NE England produced 300 000 m^3 of brine and 100 m^3 of Carboniferous-derived oils through the Permian salt over a 1 year period. Evaporite beds are the most effective seal in a hydrocarbon system, but they are not a perfect seal and commercial volumes of hydrocarbons can occasionally migrate through salt over short time scales.

Evaporites are generally perceived to be the weakest lithology in a sedimentary basin and assumed to always deform only by deformation mechanisms that approximate to viscous or power-law flow (pressure solution, solid-state diffusion and dislocation creep). However, examples of brittle faulting in evaporites do occur in very localized areas in some mines and surface exposures of salt domes and extrusions. This paper reviews these rare examples of natural faulting in salt, and briefly summarizes what is known about brittle deformation and fluid flow through salt from laboratory studies. Many of the faults in salt are disguised by later ductile shearing, so that shear zones are developed that contain vestiges of the original faulting such as breccia zones with rounded fragments and sheared veins associated with fluid flow. Such palaeo-faulted intervals have been documented in natural diapirs in Oman where oil is leaking from large anhydrite inclusions within the salt, and from the salt itself, which had lost its sealing capacity (Schoenherr & Urai 2007; Schoenherr *et al*. 2007). These ‘anomalous’ zones exhibit unusually large grain-size salt with high gas and fluid content, and oil and bitumen staining (Kupfer 1962, 1976, 1990; Neal *et al*. 1993; Ehgartner *et al*. 1998). ‘Anomalous’ zones can cause gas outbursts into salt mines during mining operations, which create large inverted funnel-shaped caverns in the roof of mine galleries that can have volumes up to 45 000 m^3 (Fig. 1, Ehgartner *et al*. 1998; Menzengraben, potash mine no. 3, southern Harz region, Gimm 1968). The gas outbursts can contain methane, carbon dioxide, hydrogen sulphide, and nitrogen (Baar 1977), which have been responsible for miners’ deaths both down the mine and at the surface, where CO_2 outbursts have ponded in topographic depressions. Several mines have been abandoned because of the high number of casualties (Baar 1977).

Brittle deformation mechanics of halite

Laboratory experiments on halite indicate that it deforms in a brittle manner when the strain rate increases to a critical level and salt enters the dilatancy domain (e.g. Spiers *et al*. 1989; Thorel & Ghoreychi 1996; Critescu & Hunsche 1998). At a confining pressure of 25 MPa (equivalent to 1 km of burial), failure occurs at differential stresses greater than 25 MPa (Fig. 2). Using the viscous steady-state creep law of Critescu & Hunsche (1998, p. 51, table 2.2, second law) for dry salt deforming at a temperature of 50 °C with a differential stress of 25 MPa, the strain rate at brittle failure would be $5 \times 10^{-9}\ s^{-1}$. This is a very high strain rate, which could be caused by earthquake shocks (see below) but is unlikely to occur in most normal salt tectonic settings, where strain rates rarely exceed $10^{-12}\ s^{-1}$. However, where the pore fluid is overpressured and the effective stress is low, salt will fault at much lower differential stress and strain rates (Schleder *et al*. 2007).

High stresses, strain rates and fluid pressures in naturally deformed salt

As salt is most likely to fault when the effective stresses are relatively low (Critescu & Hunsche 1998) it is worth examining how large fluid pressures build up in salt.

High fluid pressures

Fluid pressures close to lithostatic pressures are common in salt and this contributes to faulting and hydraulic fracturing (Schleder *et al*. 2007; Schoenherr *et al*. 2007). Fluid pressures build up in evaporites undergoing burial through important metamorphic reaction thresholds such as the transition from gypsum to anhydrite, which releases bound water from the crystal structure ($CaSO_4.2H_2O \rightarrow CaSO_4 + 2H_2O$) and can increase the volume of the system by a factor of 38% (gypsum molar volume 74.7 $cm^3\ mol^{-1}$ and anhydrite molar volume 46 $cm^3\ mol^{-1}$). This transition occurs at depths from several metres to several kilometres depending on various parameters such as pore fluid salinity, pore fluid pressure, salt composition, grain size and geothermal gradient. The gypsum anhydrite conversion has been observed to occur between 70 and 105 °C (Hardie 1967; Jowett *et al*. 1993). Hence, when salt layers are buried to depths of 2–3 km any included gypsum will dehydrate and the liberated fluid

Fig. 1. A large inverted funnel shaped cavern produced by gas outburst in halite from a mine gallery roof in the Weeks Island Salt Dome, Gulf Coast of Mexico. After Acres American Inc. (1978).

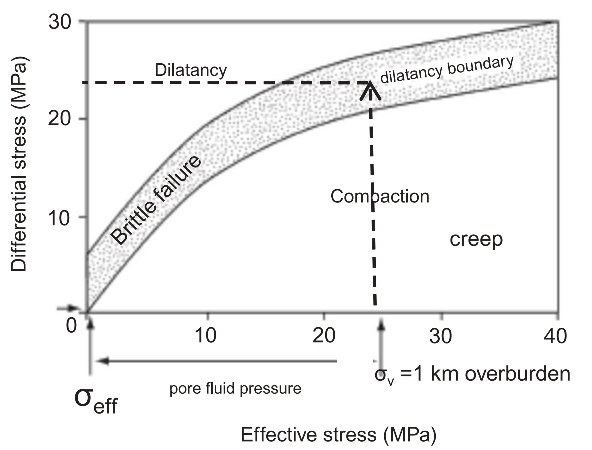

Fig. 2. Plot of effective stress v. differential stress showing dilatancy and compaction stability fields of salt. An overburden stress of *c*. 25 MPa occurs at depths of 1 km in salt, which requires a differential stress of *c*. 24 MPa to produce dilatancy in salt. Adapted from Popp *et al*. (2001) and Schleder *et al*. (2007).

is likely to hydraulically fracture a temporary migration pathway out of the salt, which usually then reseals. The other main volume-changing reaction in evaporite sequences is the carnallite to sylvite transition ($KMgCl_3.6H_2O + 4\,H_2O \rightarrow KCl + Mg^{2+}\ 2Cl^- + 10H_2O$). This reaction involves volumetric increases of 40% (estimated by Schleder *et al*. 2007). This can cause large-scale fluid escape from the carnallite layer. High fluid pressures created by metamorphic reactions can cause diffuse dilatancy, leading to the formation of interconnected fracture networks that greatly increase permeability (e.g. Connolly *et al*. 1997; Holness & Watt 2002).

Generation of oil and gas from shales included within the evaporite sequence also creates large volume increases that lead to fluid overpressure. The fracturing in the Pugwash, Magdelen and Gorleben salt mines described below is thought to be caused by maturation of organic shales.

Even in the absence of dilatancy, the juxtaposition of brines and a brine-free rock can result in spontaneous fluid infiltration driven by the resultant decrease in the total internal energy of the system (M. Holness, pers. comm.). This is because the low dihedral angle ($<60°$) in the water–halite system stabilizes an interconnected network of fluid-filled channels along grain boundaries where three grains meet (Lewis & Holness 1996; Holness & Lewis 1997). This is a lower energy configuration compared with an initially brine-free halite (M. Holness, pers. comm.).

Lewis & Holness (1996) showed that at temperatures >100 °C and pressures of 70 MPa the brine–halite dihedral angle is less than the critical value (60°) which favours the stabilization of the grain-edge channels. The resultant increase in permeability reaches millidarcy levels. Schleder *et al*. (2007) calculated that this level of hydrostatic stress would occur at 3–4 km depth.

High stresses and rapid strain rates in salt

In general, differential stress is low in stable salt. For example, Schoenherr *et al*. (2007) have measured the differential stress in a salt mine within a stable buried salt body using sub-grain sizes and concluded that the maximum differential stress ($\sigma_1 - \sigma_3$) is less than 2 MPa, indicating that this is a nearly uniform stress field (see also Carter *et al*. (1993) and Franssen (1993) with other worldwide observations). However, in certain situations stresses become concentrated in sedimentary basins and promote rapid deformation. The locations where salt is highly stressed are generally in the following situations: salt diapirs; at shallow structural levels in rapidly spreading salt extrusions; detachments and along active listric growth faults that sole down into the salt; above active faults that propagate upwards into the salt layer; in zones of rapid salt thickness change at basin margins and over faulted blocks (Figs 3 and 4).

Salt diapirs. At high stress levels, which produce rapid strain rates, salt can be stronger than shallow-buried unlithified sediment, and it is only after several metres to hundreds of metres of burial that the salt will become weaker than the partially consolidated overburden sediment. This is important, as many diapirs grow by downbuilding where the crest of the salt diapir remains near the sediment surface over long periods of time, and where any weak overburden sediments deposited over the diapir may then slump off (e.g. Davison *et al*. 2000).

Where buoyancy forces or regional tectonic compression produce active salt dome uplift, the top salt surface moves upward in relation to the geoid. For example, the Weeks Island Dome, Gulf Coast of Mexico, has uplifted capping sediments by

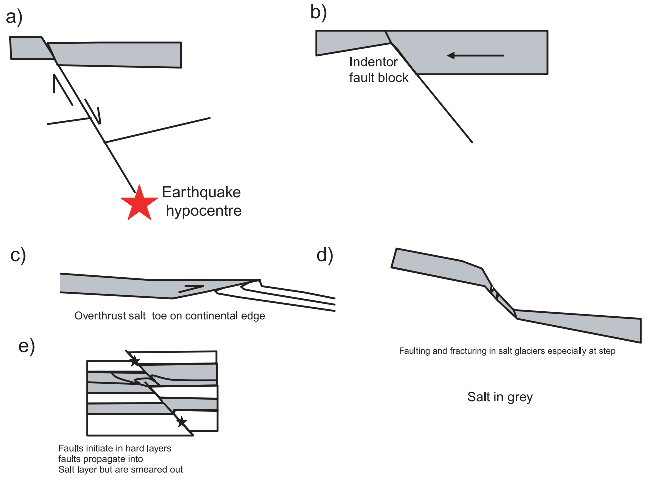

Fig. 3. Sketch illustrating possible situations where high stress build-up occurs in salt layers in sedimentary basins. (**a**) Earthquake propagating up from mid-crustal depths through salt layer. (**b**) Fault produced above indenting rift block below salt. (**c**) Rapid flow over unconfined salt at the sediment surface. (**d**) Rapid change in salt thickness and slope on base of salt extrusion. (**e**) Smaller faults propagating from interbedded more competent layers within the evaporite sequence.

50 m in last 25 000 years, equivalent to 2 mm a^{-1} (Neal *et al.* 1993); the Mount Sedom diapir, Dead Sea, has uplifted at a rate of 6–7 mm a^{-1} over the last 8000 years (Frumkin 1996); the Al Salif diapir in Yemen has uplifted at a rate of 4.6 mm a^{-1} over the last 3700 years (Davison *et al.* 1996); and Qum Kuh in Iran at present extrudes at 82 mm a^{-1} (Talbot & Aftabi 2004). The last example is the most rapid, and is equivalent to a vertical strain rate of *c.* 6.4×10^{-12} s^{-1}. This is lower than the strain rates that might fault the salt (see above). Strain rates are calculated as per cent linear strain per second; that is, ((final length − original length)/original length × 100).

Salt glaciers. Salt glaciers are surface extrusions of salt where the salt is fountaining from a diapir stem and flowing over the Earth's surface. The flow rates in the Iranian salt glaciers have been extensively studied by Talbot & Rogers (1980), Talbot (1998), Talbot *et al.* (2000), Talbot & Aftabi (2004) and Aftabi *et al.* (2005). The Kuh e Namak (Dashti) salt glacier flowed more than 1 m in 2 days after heavy rainfall (Talbot & Rogers 1980). The Kuh-e-Jahani salt glacier is rising out of its orifice at 2–3 m a^{-1} (Talbot *et al.* 2000), which is equivalent to a vertical strain rate of 1×10^{-11} s^{-1}. This is close to the critical strain rate for salt to fault. The submarine salt sheets beneath the Gulf Coast of Mexico flowed downslope at time-averaged rates between 1.5 and 275 mm a^{-1} from Miocene to Pliocene time (Wu *et al.* 1990; quoted by Talbot 1998). This time-averaged rate is equivalent to a horizontal strain rate of *c.* 1×10^{-12} s^{-1} for a 10 km wide salt sheet. These rates are below the critical strain rate for brittle fracture of salt.

Basal detachments. The rates at which rafts of Albian carbonate slid downslope over Aptian salt off the shore of the West African Atlantic margin have been constrained by Rouby *et al.* (2003). They estimated a maximum displacement rate of 2200 m Ma^{-1}, which is equivalent to a horizontal strain rate of 1.5×10^{-14} s^{-1} assuming a 25 km long system averaged over a 10 Ma period. This is slower than the rate at which faulting would occur in the salt, but wherever there is a step in the basal detachment and the salt suddenly changes thickness, the strain rate will increase by an order of magnitude or more and may cause faulting.

Active basement faulting propagating up through a salt layer. Wherever active faults are propagating up from the basement into salt structures, major faults can be expected to displace the sedimentary layers by several tens of centimetres to metres in a few seconds. The salt will respond by brittle faulting, where the fault tip is propagating at seismic velocities (3–4 km s^{-1}). The ground surface over the crest of a large salt diapir on the Greek island of Strophades was ruptured by a co-seismic vertical thrust with a displacement of 10 cm and a strike-slip movement of 12 cm during the M_W 6.5 earthquake on 18 November 1997 (Stiros 2005). The hypocentre of the earthquake was estimated at 32 ± 3 km depth; this is well below the evaporite layer and indicates that the fault propagated up through the salt diapir, which is estimated to be several kilometres in height (Stiros 2005).

The Gulf of Suez and northern Red Sea area onshore Egypt are undergoing active extensional tectonics. Historical newspaper articles have documented earthquake displacements on normal faults rupturing the ground surface and causing small (<1 m fault scarps) to develop (W. Bosworth, pers. comm.). The fact that these areas in Egypt are underlain by continuous salt layers strongly suggests that the salt layer has also been faulted, as the earthquakes are propagating from focal depths of *c.* 10–15 km (Jackson *et al.* 1988).

Examples of natural faults, tensional fractures and veins in evaporites

Boulby Mine

The Boulby Mine is located in a Zechstein evaporite sequence in the Cleveland Basin of northern England, which forms the

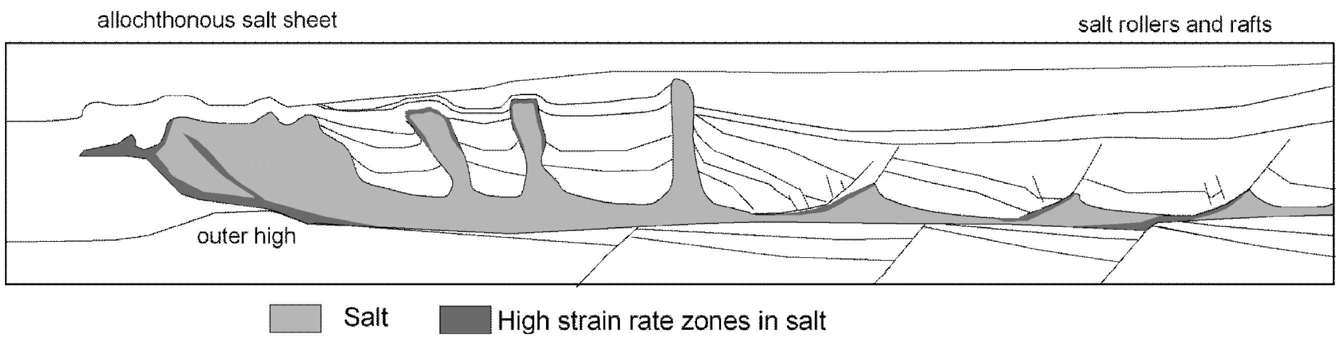

Fig. 4. Schematic section of salt structures on a continental margin showing high strain rate zones where salt is more likely to undergo brittle faulting.

western margin of the North Sea Basin (Talbot *et al*. 1982; Botterell *et al*. 1996). The mine workings reach a depth of 1.3 km below sea level and extend some 8 km beyond the coast beneath the North Sea. The Zechstein sequence consists of cycles of dolomite, anhydrite, halite, carnallite and shale. Normal faults were produced during a phase of post-Triassic extension that cut the salt layer (Fig. 5), but the faults are probably reactivated Carboniferous rift faults. The offset of the top salt is *c*. 300 m, but at base salt there is very little offset. There may have been some dissolution of the salt in the hanging wall of the fault, where the Zechstein layer is noticeably thinner (Fig. 5).

Thrust faults have also been produced by basin inversion of post-Triassic age. The actual age of inversion is difficult to determine exactly but it is thought to have occurred during the Cenozoic, when regional uplift and denudation occurred in the area (Menpes & Hillis 1996). A thrust fault with *c*. 17 m of displacement has been mapped in Panel 600, which probably nucleated in the dolomite layers and propagated and dissipated through into the evaporite layers. The evaporites show intense mylonitic shearing fabrics adjacent to the fault plane (Fig. 6), and the grain size of the salt increases from 4 mm average to 8 mm in the vicinity of the fault and the grain flattening in the *xz*-plane of the strain ellipse reaches 6:1. The mylonitization dies out rapidly in the evaporites and the Boulby Halite decreases in thickness from 33 m in the footwall of the fault to 12 m in the hanging wall (Fig. 6a). Further along in Panel 600, there are zones with many dilational veins of up to 10 cm width (Fig. 7a), which are filled with euhedral sylvite crystals (Fig. 7b). These veins are in several orientations (including horizontal) and indicate that fluid pressures rose to exceed the lithostatic pressure. The 2–5 cm wide veins must have been propped open by migrating fluids to allow the euhedral cubic crystals to grow.

The mine gallery in Panel 572 intersected fluids migrating along fracture surfaces. The first brine influx occurred from an old 5 cm wide exploratory horizontal borehole drilled through the salt. The roof to floor closure increased soon after this, and after 2 weeks fluids started to flow directly up through fractures induced by the mining operation as they widened by fluid dissolution. The fractures produced *c*. 300 000 m^3 of brine over a 1 year period (Holmes 2001; R. Holmes, pers. comm.). This produced a brine pool on the floor of the mine gallery that had to be pumped out to the surface (Fig. 8). An estimated 100 m^3 of oil and an unquantified amount of methane gas were also produced in the first year. The flow still persists 10 years later, but at a much slower rate of several litres per day. The oil has been analysed and was linked to the Carboniferous land plant kerogen types of the Coal Measures (C. Cornford, pers comm.). The mine gallery is situated around 200 m above the base of the Permian salt sequence, indicating that open fractures are cutting through at least this amount of rock to reach the mine gallery. The mine gallery is an artificial opening, and the faulting and fracturing were induced by the high stress concentration around this rapidly opened void. However, this example indicates how faults and fractures can permit large fluid volumes to migrate through a thick salt sequence (several tens to hundreds of metres).

Aptian age salt in Brazil

Taquari–Vassouras Potash Mine (Aracaju), Sergipe–Alagoas Basin, NE Brazil

The Companhia Vale Rio Doce (CVRD) Taquari–Vassouras Potash Mine, Sergipe State, Brazil Mine near Aracaju is situated at *c*. 300 m below the ground surface in the Sergipe–Alagoas Basin of NE Brazil (Carvalho *et al*. 1995; Machado & Szatmari 2008). The late Aptian evaporites (*c*. 114-116 Ma) are affected by numerous small thrusts (<1.5 mm displacement (Fig. 9b) and probable strike-slip faults (Fig. 9a) which affect the halite, carnallite, siltstone and organic shale layers. Carnallite is much weaker and more ductile than halite, but this is also faulted in the example shown in Figure 9a. The age of the faulting is not

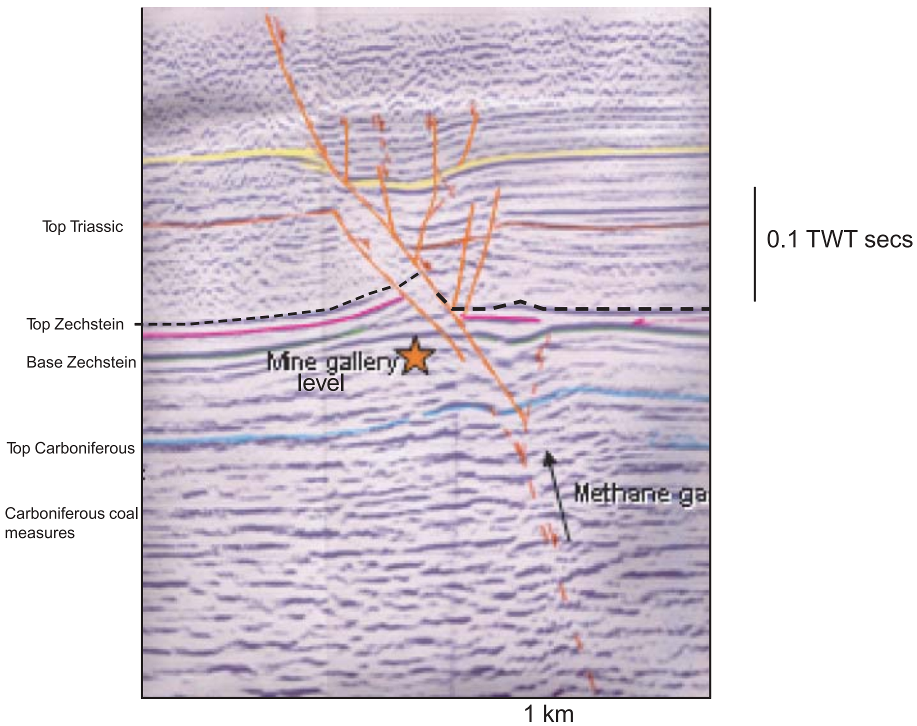

Fig. 5. Seismic section several kilometres south of the Boulby Mine, showing an oblique extensional fault cutting through Zechstein sequence and equivalent approximate level of mine gallery. The top and base salt horizons are offset by the faulting. TWT, two-way travel time.

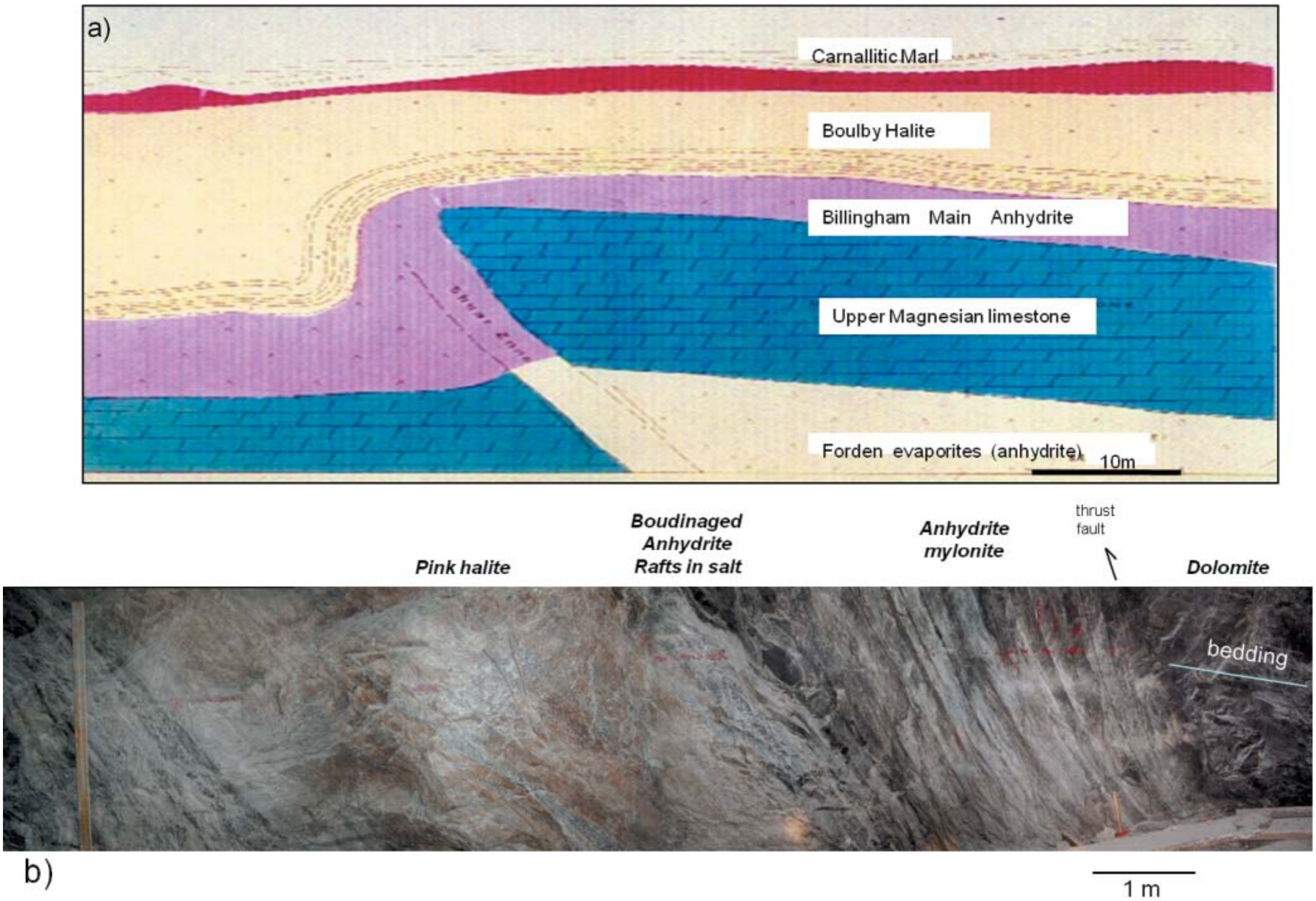

Fig. 6. (**a**) Geological section through thrust fault in Panel 600. After R. Holmes (unpubl. data). (**b**) Photograph of same fault as in (**a**), which affected the Upper Magnesian Limestone in the Zechstein sequence. The fault dies out very quickly into the overlying Billingham main anhydrite and Boulby halite.

known but it probably occurred in Cretaceous times, when large-scale extensional faults continued to be active after salt deposition. The fault planes are commonly filled with euhedral dark grey halite crystals. Open dilation fractures have developed in the salt, which are at a depth of 540 m (Carvalho *et al*. 1995). The fractures trend 030° and are parallel to small-scale anticlinal fold hinges.

Occasionally, the fault planes have isolated voids up to 6 cm wide, which contain overpressured methane gas and are rimmed by euhedral cubic halite crystals up to 2 cm in diameter (Fig. 9c). These have been known to cause catastrophic outbursts when mined (A. Carvalho, pers. comm.). The methane gas was probably generated from an interbedded organic-rich source that is currently mature for oil and gas generation in the offshore area but is immature onshore in the region of the mine.

Salt in Santos Basin, Brazil

High-resolution seismic data from the central Santos Basin indicate that the late Aptian age salt layers are faulted by normal faults (Fig. 10, Freitas 2006). The faults offset the internal reflections within the salt body by *c*. 10 m and they cut through all the tachydrite, halite, carnallite and anhydrite layers. The age of the faulting is not known, but the faults offset the top salt horizon and the Albian carbonates, indicating that it is post-Albian.

Carboniferous age salt in Nova Scotia

Pugwash salt diapir

The Pugwash salt diapir in Novas Scotia is a >2 km high structure of Carboniferous (Viséan) age halite and interbedded anhydrite units that have been highly deformed by halokinesis during the late Carboniferous period (Evans 1965; Carter 1990). Two small faults have been observed in the mine galleries at depths of *c*. 250 m (830 foot level) (Fig. 11; B. Wile, pers. comm.). One fault has a normal displacement sense, with clear offset of bedding by several tens of centimetres (Fig. 11). Polished slickenside surfaces are present in the salt along the fault plane with scratched striae markings. The fault has a slow oil seep (several litres per month) associated with it, which was active for several years before drying up (B. Wile, pers. comm.). The fault zone has associated veins of blue euhedral halite. This unusual coloured halite is thought to be due to the presence of numerous fluid inclusions (geochemical analysis did not reveal any detectable salt impurities). Oil seepage sourced from the Macumber Limestone Formation located near the base of the Windsor salt interval (tens of litres per year) indicates that fluid movement has taken place over several years.

Magdalen Island salt mine

The Magdalen Island Mines Seleine salt dome on Gros Isle, Quebec, is composed of Viséan age salt (Fig. 12). The salt contains

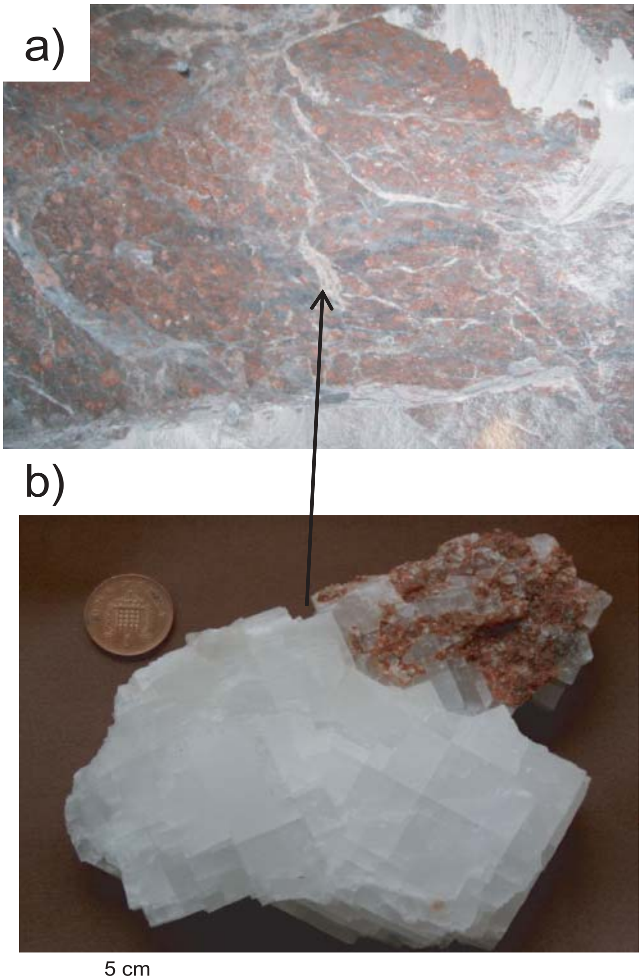

Fig. 7. (**a**) Tensional vein network in sylvinite in Panel 600. Veins are filled with sylvite. (**b**) Close-up of euhedral cubic crystals of sylvite in tensional veins indicating that the veins were open voids during sylvite crystallization, which were held open by fluids at supra-lithostatic pressures.

fluid inclusions that contain oil and gas, indicating fluid flow through the salt (Zentilli *et al*. 2008). Brecciated zones of halite with vein infill of pink halite and sylvinite occur on level 3 of the mine at a depth of −223 m (M. Zentilli, pers. comm.). This type of 'explosive' brecciation is strongly suggestive of high overpressure built up within the salt, which has provoked the fracturing.

Iranian salt

Fracturing in the Qum Kuh salt extrusion

The Qum Kuh salt diapir is currently producing a surface glacier that is extruding at a rate estimated at 82 mm a^{-1} (Talbot & Aftabi 2004; Aftabi *et al*. 2005). This equates to a strain rate of *c*. 8×10^{-13} s^{-1}. This relatively rapid rate of extrusion is due to the continental collision occurring in central Iran. The outward radial flow of salt away and downslope from the extrusive orifice has caused both radial and concentric brittle fracturing of the salt (Talbot & Aftabi 2004). The fractures are widest (less than a few centimetres) within 10 cm of the salt surface, and some of the largest taper downwards for at least 30 m below the salt surface (Fig. 13c). Some joints extend over several hundred metres laterally and these probably extend much deeper (>100 m) into the Qum Kuh glacier. Both radial and concentric fractures have been mapped in a systematic pattern indicating the 3D expansion of the top salt surface flowing away from crest of the dome (Fig. 13a and b).

Faulting in the Eivanekey plateau in Central Iran

Faults are common along the eastern margin of the Eivanekey plateau in front of the advancing Alborz Mountains. Two exposed fault surfaces in halite in a Cenozoic age salt quarry several metres below ground surface show transcurrent slick-enlines, indicating frictional wear and tooling of harder grains in the salt (Fig. 13d).

Gorleben salt diapir, northern Germany

The Gorleben salt diapir in northern Germany is one of the most studied salt domes in the world as it has been used as a research

Fig. 8. Brine pool on the floor of the Boulby mine gallery caused by fluid infiltration along a mining-induced fracture. This fault produced 300 000 m^3 of brine fluid over a 1 year period together with a small amount of oil derived from underlying Carboniferous source rocks.

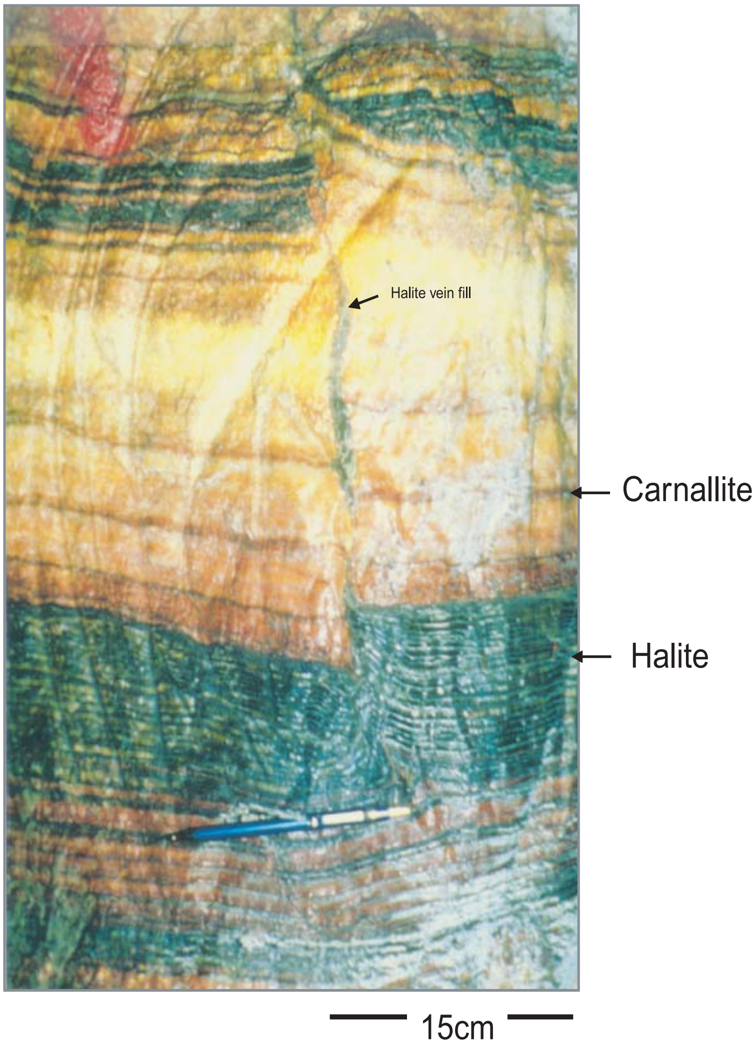

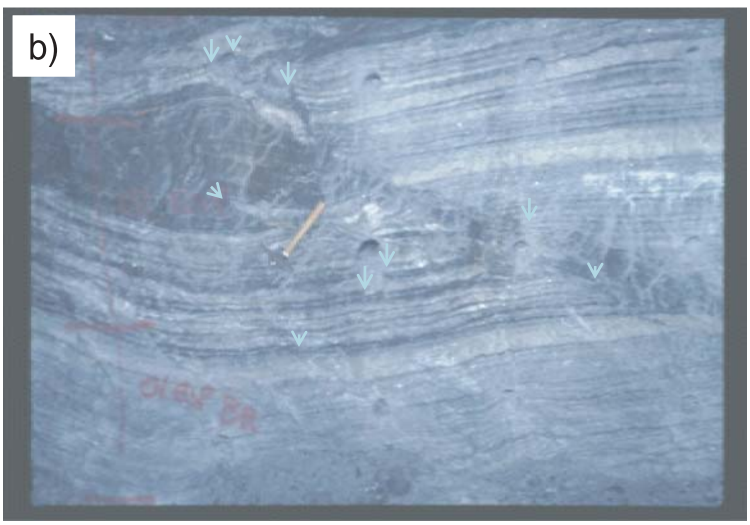

Fig. 9. (**a**) Strike-slip fault in CVRD Taquari–Vassouras Potash Mine, Sergipe near Aracaju in the Sergipe–Alagoas Basin, NE Brazil. The faults are truncating both halite and carnallite layers, with recrystallized coarse-grained dark grey euhedral halite crystals present along the fault plane (arrowed). (**b**) Thrust faults in same mine; dark-coloured recrystallized cubic halite crystals along the fault planes. Fault planes are indicated by light-coloured arrowheads. (**c**) Open fracture in halite rimmed with euhedral cubic halite crystals. Methane outbursts from these open fractures have killed miners in the past (A. Carvalho, pers. comm.).

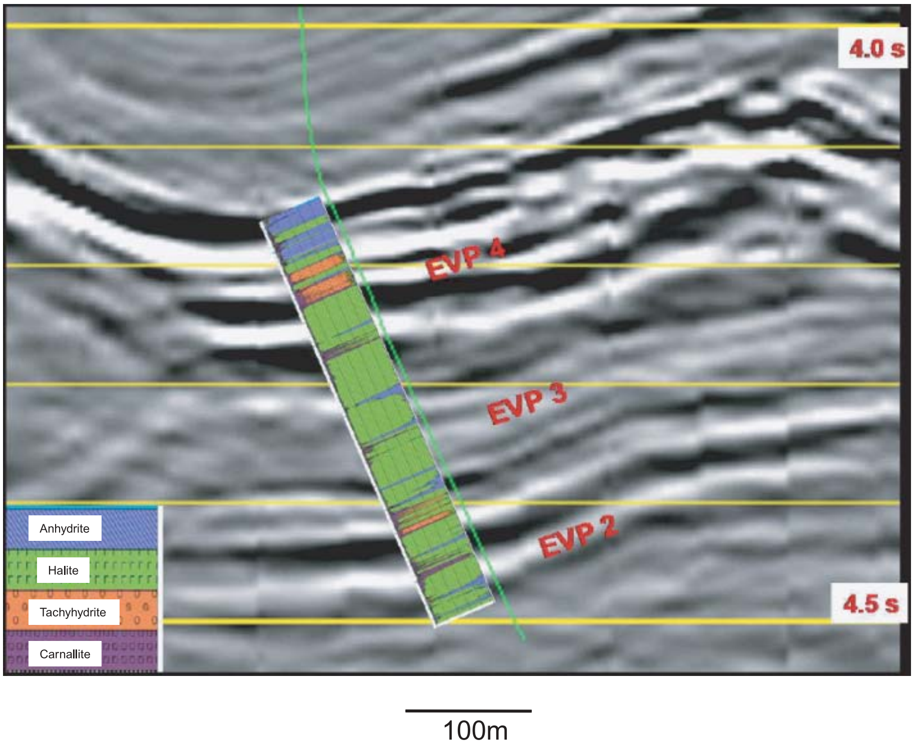

Fig. 10. Seismic section though well RJS-598D in the Santos Basin, Brazil. Salt layering is offset by many small faults with *c*. 10–20 m displacement. Vertical scale in two-way travel time seconds (from Freitas 2006).

Fig. 11. Fault in Carboniferous age halite layers in the wall exposure of Pugwash Salt Mine, Windsor Salt Company, Pugwash, Nova Scotia. Recrystallized cubic halite crystals up to several centimetres in diameter are present along the fault plane. Oil seeps occurred for *c*. 2 years along this fault.

mine for studying the possibility of storing nuclear waste (Bornemann 1991; Zirngast 1996). The detailed mine mapping (Bornemann 1991) indicates zones of intense shearing where large competent sections of the Zechstein stratigraphy are locally missing. In one of these zones a 2–5 m wide zone of breccia is observed in mine galleries 800 m deep. This is interpreted by the author as a sheared breccia zone where angular fragments have been broken and subsequently sheared and rounded to give a mixed mylonite–breccia zone (Fig. 14a). One of the outer edges of the sheared zone has a knife-sharp planar contact with the less deformed halite that exhibits all the attributes of a brittle fault plane (Fig. 14a). There are also zones *c*. 2–3 m wide that are more permeable and porous than normal salt, and oil is slowly oozing from the mine gallery walls at a rate of several tens of litres per year (Fig. 14b). Both the fault zone in Figure 14a and the oil-stained zone (outlined with black paint lines in Fig. 14b) are oriented parallel to bedding.

Gulf Coast of Mexico salt domes

Anomalous sheared and faulted zones have been described from several onshore salt domes in the Gulf Coast of Mexico (Kupfer 1962, 1976, 1990; Neal *et al*. 1993). One shear zone in the Big Hill Dome crosses the entire salt stock and links to a graben-forming fault in the overlying cap rock (Neal *et al*. 1993). These ‘anomalous’ zones are characterized by the following: (1) increased shearing, faulting and slickensides; (2) increased salt porosity and permeability; (3) reduced density and sonic velocity of salt; (4) halite recrystallization; (5) seeps of brine or hydrocarbons; (6) association with gas outbursts; (7) variable colours of salt (Balk 1949; Muehlberger 1960; Kupfer 1990; Neal *et al*. 1993).

The zones can be up to 100 m wide and their long dimension can be the whole width of the salt dome (although the 3D shape has not yet been determined because of the lack of 3D control in the salt domes). Some 150 barrels of liquid hydrocarbons were

Table 1. *Summary of evidence for faulting in evaporite sequences*

Basin and locality	Evidence	Displacement	Reference
Northern Red Sea	Earthquake faulting propagated from pre-salt basement causing 1 m offset of beach terraces at surface	Normal 1 m	W. Bosworth (pers. comm.)
Nova Scotia Maritimes Carboniferous Basin, Pugwash Mine	Faults in salt mine at 600 m depth with euhedral blue halite crystals and oil staining and striae along fault plane	Normal fault <0.5 m apparent displacement	This paper
Sergipe–Alagoas Basin, NE Brazil	Numerous thrust and strike-slip faults with methane migration along open fault planes or recrystallized halite crystals	Thrust and strike-slip <1 m displacement	This paper and Carvalho *et al*. (1995)
Boulby Mine, Cleveland Basin, Zechstein, NE England	Thrust fault in mine gallery	10 m	This paper and R. Holmes (unpubl. data)
Strophades, West Hellenic arc	Offset of ground surface	Co-seismic thrust 10 cm, strike-slip 12 cm	Stiros (2005)
Kuh e Namaq, Zagros Mountains, Iran; Eivaneky plateau, Alborz Mts	Radial and concentric tensional fracturing in salt surface exposures; faults with slickenlines in salt quarry	Maximum *c*. 10 cm tensional opening	Talbot & Aftabi (2004)
Werra Salt, German Zechstein basin	Faults in overburden linked to shear zones and sink holes	Normal metre scale	Schilder & Schwandt (1983)

Fig. 12. Brecciated salt (dark) and vein infill of reddened halite with iron staining and sylvinite, from Magdalen Island Mines Seleine, Quebec. Courtesy of M. Zentilli.

produced from a shear zone in the Big Hill salt stock in leached cavern 114 (Neal *et al*. 1993). In the Weeks Island Dome, a methane gas outburst from an anomalous zone produced 50 million cubic feet of gas into the Morton Mine (see Fig. 1; Ehgartner *et al*. 1998). This is probably thermally derived gas that has been generated from shales within the salt and trapped at lithostatic pressure in porous salt (Iannacchione & Schatzel 1985). The ejected grains of salt from the outbursts are known as popcorn salt, as they make a popping sound as one walks over them (Ehgartner *et al*. 1998).

Conclusions

Brittle faulting and fracturing, and fluid and gas flow have been observed in salt (Table 1). Laboratory experiments indicate that salt will fracture at strain rates greater than 10^{-9} s^{-1}. However, such rapid strain rates rarely occur in salt bodies, except where earthquake faulting propagates up through the salt layer. Fracturing and faulting are most likely to occur in the presence of overpressured fluids. Several examples of dilational veins are presented that are strongly indicative of fluids reaching lithostatic

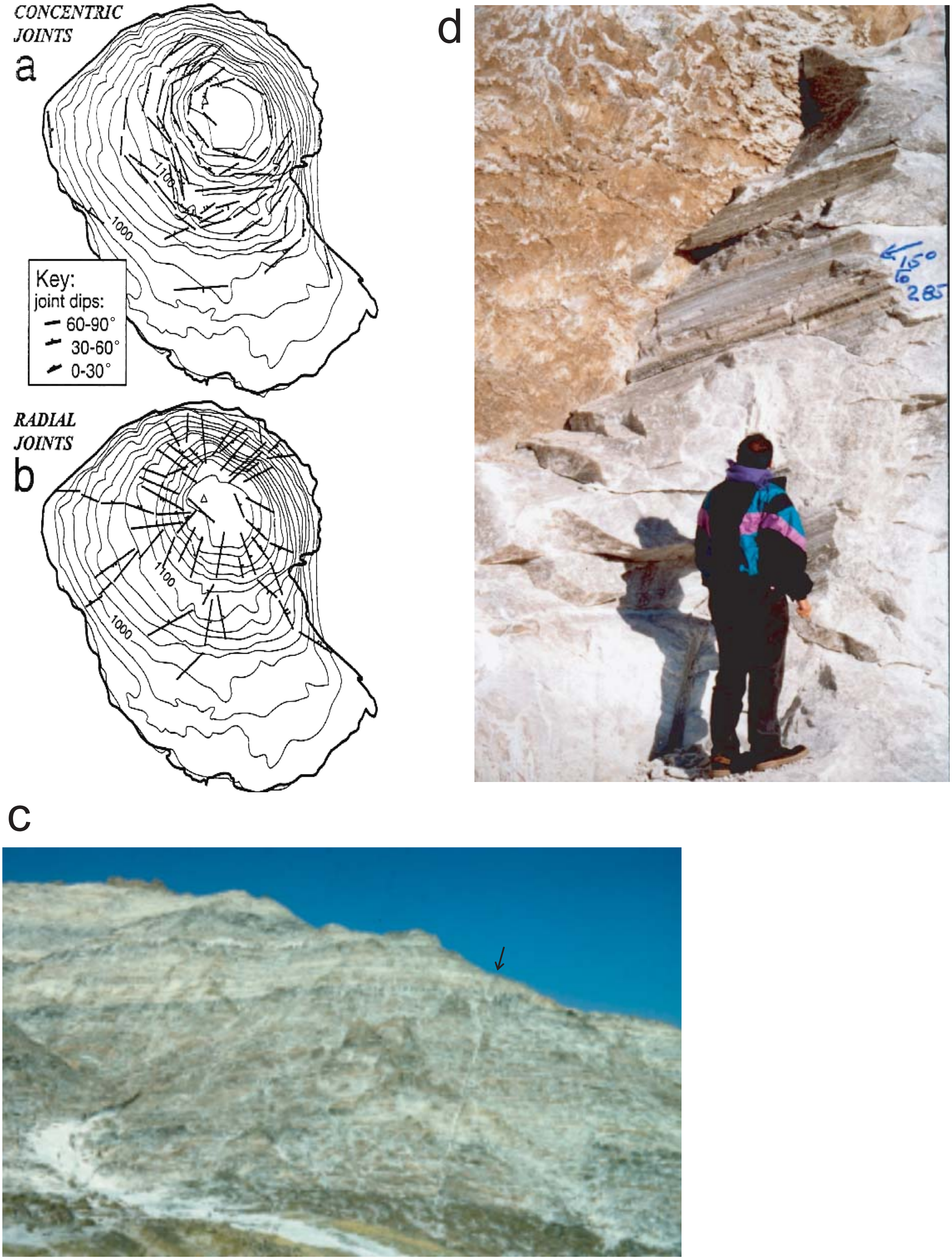

Fig. 13. Map of (**a**) concentric joints and (**b**) radial joints in the surface of the Qum Kuh salt glacier. Topographic contours are in metres. Reproduced from Talbot & Aftabi (2004). (**c**) An unusually long joint (>30 m) in the upper reaches of the southern extrusion of Kuh e Namak (Dashti). The lighter rocks in the foreground are country rocks, and the main cliff face is halite. Photo courtesy of C. Talbot. (**d**) Two exposed fault surfaces in halite in a Cenozoic age salt quarry several metres below ground surface at the SE edge of the Eivanekey plateau in Central Iran. Slickenlines on fault surface are covered in brown clay. Faults like these are common along the eastern margin of the plateau in front of the advancing Alborz Mountains. Photo courtesy of C. Talbot.

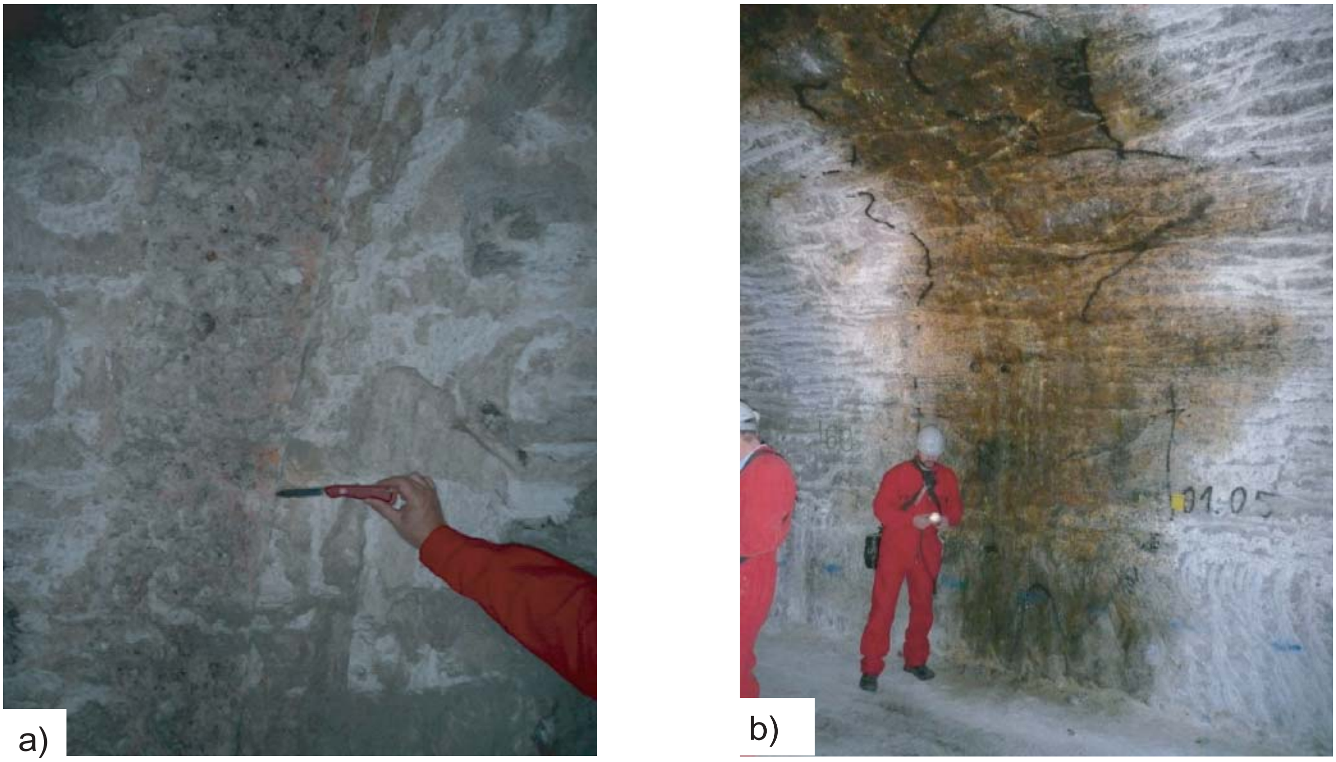

Fig. 14. (**a**) Photograph of brecciated fault zone in Gorleben mine, northern Germany. Breccia fragments are interpreted to be rounded as a result of ductile deformation after fracturing. (**b**) Oil-stained shear zone in Gorleben. The bedding and shear zone fabric is vertical. Zone of oil staining has been outlined with black paint lines. Horizontal tool marks caused by mining operations are also visible.

pressure. Faults are observed even in carnallite, which is much more ductile than halite. The faults can be open for 10 years or more when high pressure fluid is maintained. This can be enough time to allow transport of commercial volumes of hydrocarbons through salt layers. Salt is the best hydraulic seal in a sedimentary basin but it is not a perfect seal. Fluids can migrate either along grain boundaries at depths of *c*. 3–4 km or through faults and fractures, which are usually induced by high fluid overpresssure created by metamorphic reactions in the evaporite sequence.

I thank R. Holmes for providing information on the Boulby Mine, and Cleveland Potash Ltd for permission to publish these data. C. Talbot provided a very helpful and thorough review of this paper and Figure 13. O. Schulze, J. Urai and M. Holness kindly led me through the labyrinth of salt creep laws and failure criteria. M. Zentilli provided the photograph from the Magdalen Island salt mine.

References

Acres, American Inc. 1978. *Photographs of the Weeks Island Mines*. Courtesy of Stewart Thompson. Contract DEA-121-75, Gulf Interstate Engineering Company for the US Federal Energy Administration, Buffalo, NY.

Aftabi, P., Talbot, C.J. & Fielding, E.J. 2005. Salt kinematics and in SAR. *In: Radar Investigations of Planetary and Terrestrial Environments (Abstracts)*. Lunar and Planetary Sciences Institute, Houston, TX, 17.

Baar, C.A. 1977. *Applied Salt Rock Mechanics, 1: the* In-situ *Behaviour of Salt Rocks*. Developments in Geotechnical Engineering, **16A**.

Balk, R. 1949. Structure of the grand saline dome, Van Zandt Co., TX. *AAPG Bulletin*, **37**, 2455–2477.

Bornemann, O. 1991. *Zur Geologie des Salzstocks Gorleben nach den Bohrergebnissen*. Bundesamt fur Strahlenschutz, Salzgitter, **4/91**.

Botterell, S.H., Leosson, M.A. & Newton, R.J. 1996. Origin of brine inflows at Boulby potash mine, Cleveland, England. *Transactions Section B, Applied Earth Science*, **105**, 159–164.

Carter, D.C. 1990. *Map 90-3, Geology of the Canadian Salt Company Limited, Pugwash Mine (11E/13) 830 level, Pugwash, Nova Scotia. Scale 1:1600*. Department of Mines and Energy, Halifax, Nova Scotia.

Carter, N.L. & Hansen, F.D. 1983. Creep of rock salt. *Tectonophysics*, **92**, 275–333.

Carter, N.L., Horsman, S.T., Russel, J.E. & Handin, J. 1993. Rheology of rocksalt. *Journal of Structural Geology*, **15**, 1257–1271.

Carvalho, A.L.P., lves, E. & Padua, A.C. 1995. Geology of the Taquari–Vassouras Potash Mine, Sergipe State, Brazil. *SME Annual Meeting, Denver, Colorado, Society for Mining, Metallurgy and Exploration, Inc., Preprints*, **95-177**.

Connolly, J.A.D., Holness, M.B., Rubie, D.C. & Rushmer, T. 1997. Reaction-induced microcracking: an experimental investigation of a mechanism for enhancing anatectic melt extraction. *Geology*, **25**, 591–594.

Critescu, N. & Hunsche, U. 1998. *Time Effects in Rock Mechanics. Series a: Materials, Modelling and Computation*. Wiley, Chichester.

Davison, I., Bosence, D., Alsop, G.I. & Al-Aawah, M.H. 1996. Deformation and sedimentation around active Miocene salt diapirs on the Tihama Plain, northwest Yemen. *In:* Alsop, G.I., Blundell, D. & Davison, I. (eds) *Salt Tectonics*. Geological Society, London, Special Publications, **100**, 23–40.

Davison, I., Alsop, I., Evans, N. & Safaricz, M. 2000. Overburden deformation patterns and mechanism of salt diapir penetration. *Marine and Petroleum Geology*, **17**, 601–618.

Ehgartner, B., Neal, J. & Hinkebein, T. 1998. *Gas releases in salt*. Sandia National Laboratories Report, Albuquerque, New Mexico and Livermore, California. Unlimited Release Report, **SAND 98-1354**.

Evans, R. 1965. *The structure of salt deposits at Pugwash, Nova Scotia (Canada)*. MSc thesis, Dalhousie University, Halifax, N.S.

Franssen, R.C.M.W. 1993. *Rheology of synthetic rocksalt with emphasis on the influence of deformation history and geometry on the flow behaviour*. PhD thesis, Rijksuniversiteit Utrecht.

Freitas, R.T.J. 2006. *Ciclos deposicionais evaporiticos da bacia de Santos: uma analise cicloestratigrafica a partir de dados de 2 pocos e de tracos de sismica*. MSc thesis, Universidade Federal do Rio Grande do Sul, Instituto de Geociencias, Porto Alegre, Brasil.

Frumkin, A. 1996. Uplift rate relative base levels of a salt diapir (Dead Sea Basin, Israel) as indicated by cave levels. *In:* Alsop, G.I., Blundell, D. &

Davison, I. (eds) *Salt Tectonics*. Geological Society, London, Special Publications, **100**, 41–48.

Gimm, W. 1968. *Kali- und Steinssalzbergbau*. VER Deutscher Verlag für Grundsoffindustrie, Leipzig.

Hardie, L.A. 1967. The gypsum–anhydrite equilibrium at one atmosphere pressure. *American Mineralogist*, **52**, 171–200.

Holmes, R. 2001. *Artesian brine and gas flows*. Internal Confidential Company Report, Cleveland Potash Ltd.

Holness, M.B. & Lewis, S. 1997. The structure of the halite–brine interface inferred from pressure and temperature variations of equilibrium dihedral angels in the halite–H_2O system. *Geochimica et Cosmochimica Acta*, **61**, 795–804.

Holness, M. & Watt, G.R. 2002. The aureole of the Traigh Bhan na Sgurra Sill, Isle of Mull: reaction-driven microcracking during pyrometamorphism. *Journal of Petrology*, **43**, 511–534.

Iannacchione, A.T. & Schatzel, S.J. 1985. Characterization of the occurrence of methane. *In: Gulf Coast Domal Salt Mines 2nd US Mine Ventilation Symposium, Reno, NV.*

Jackson, J.A., White, N.J. & Garfunkel, Z. 1988. Relations between normal-fault geometry, tilting and vertical motions in extensional terrains: an example from the southern Gulf of Suez. *Journal of Structural Geology*, **10**, 155–120.

Jowett, E.C., Cathles, L.M. & Davis, B.W. 1993. Predicting depths of gypsum dehydration in evaporitic sedimentary basins. *AAPG Bulletin*, **77**, 402–413.

Kupfer, D.H. 1962. Structure of the Morton Salt Company mine, Weeks Island Salt Dome, Louisiana. *AAPG Bulletin*, **46**, 1460–1467.

Kupfer, D.H. 1976. Shear zones inside Gulf Coast salt stocks help to delineate spines of movement. *AAPG Bulletin*, **60**, 1434–1447.

Kupfer, D.H. 1990. Anomalous features in the Five Islands salt stocks, Louisiana. *Gulf Coast Association of Geological Societies, Transactions*, **40**, 425–437.

Lewis, S. & Holness, M. 1996. Equilibrium halite–H_2O dihedral angles; high rock-salt permeability in the shallow crust? *Geology*, **24**, 431–434.

Machado, E. & Szatmari, P. 2008. A mina de Taquari–Vassouras. *In:* Mohriak, W., Szatmaari, P. & Anjos, S.M.C. (eds) *Sal: Geologia and Tectonica, Exemplos nas Bacias Brasilieras*. Beca, São Paulo, 414–423.

Menpes, R.J. & Hillis, R.R. 1996. Determining apparent exhumation from chalk outcrop samples, Cleveland Basin/East Midlands Shelf. *Geological Magazine*, **133**, 751–762.

Muehlberger, W.R. 1960. Internal structure and mode of uplift of the Grand Saline Dome, Van Zandt Co., TX, USA. *21st International Geological Congress, Copenhagen*, **18**, 28–23.

Neal, J.T., Magorian, T.R., Thoms, R.L., Autin, W.J., McCulloch, R.P., Denzler, S. & Byrne, K.O. 1993. *Anomalous zones in Gulf Coast salt domes with special reference to Big Hill, TX, and Weeks Island, LA*. Sandia National Laboratories Report, Albuquerque, New Mexico and Livermore, California. Unlimited Release Report, **SAND92-2283**.

Popp, T., Kern, H. & Schulze, O. 2001. Evolution of dilatancy and permeability in rock salt during hydrostatic compaction and triaxial deformation. *Journal of Geophysical Research*, **106**, 4061–4078.

Rouby, D., Guillocheau, F., Robin, C., Bouroullec, R., Raillard, S., Castelltort, S. & Nalpas, T. 2003. Rates of deformation of an extensional growth fault/raft system (offshore Congo, West African margin) from combined accommodation measurements and 3-D restoration. *Basin Research*, **15**, 183–200.

Schilder, C. & Schwandt, A. 1983. Zur Tektonic und Auslaugung in Kali- und Steinsalzabaugebieter. *Zeitschrift für Geologischen Wissenschaften*, **11**, 1023–1033.

Schleder, Z., Urai, J.L., Nollet, S. & Hilgers, C. 2007. Solution–precipitation creep and fluid flow in halite: a case study on Zechstein (Z1) rocksalt from Neuhof Salt mine (Germany). *International Journal of Earth Science*, **97**, 1045–1056.

Schoenherr, J. & Urai, J.L. 2007. Limits to the sealing capacity of rock salt; a case study of the infra-Cambrian Ara salt from the South Oman Basin. *AAPG Bulletin*, **91**, 1541–1557.

Schoenherr, J., Urai, J.L., Kukla, P.A., Littkre, R., Schleder, Z., Larroque, J.-M. & Newall, M. 2007. Salt: a case study of the Infra-Cambrian Ara Salt from the South Oman Salt Basin. *AAPG Bulletin*, **91**, 1541–1557.

Schulze, O. 2007. Investigations on damage and healing of rock salt. *In:* Wallner, M., Lux, K.-H., Minkley, W. & Hardy, H.R., Jr (eds) *The Mechanical Behavior of Salt. Understanding of THMC Processes in Salt, Hannover, 2007*. Taylor & Francis, London, 33–43.

Spiers, C.J., Peach, C.J., Brzesowsky, R.H., Schutjens, P.M., Liezenberg, J.L. & Zwart, H.J. 1989. *Long term rheological and transport properties of dry and wet salt rocks*. Final report, Nuclear Science and Technology, Commission of the European Communities, **EUR 11848 EN**.

Stiros, S.C. 2005. Geodetic evidence for mobilization of evaporites during the 1997 Strophades (W Hellenic Arc) MW 6.5 earthquake. *Journal of Geophysics and Engineering*, **2**, 111–117.

Talbot, C.J. 1998. Extrusions of Hormuz Salt in Iran. *In:* Blundell, D.J. & Scott, A.C. (eds) *Lyell: the Past is the Key to the Present*. Geological Society, London, Special Publications, **143**, 315–334.

Talbot, C.J. & Aftabi, P. 2004. Geology and models of salt extrusion at Qum Kuh, Central Iran. *Journal of the Geological Society, London*, **161**, 321–334.

Talbot, C.J. & Rogers, E.A. 1980. Seasonal movements in a salt glacier in Iran. *Science*, **208**, 395–397.

Talbot, C.J., Tully, C. & Woods, P.J.E. 1982. The structural geology of the Boulby (Potash) Mine. *Tectonophysics*, **85**, 167–204.

Talbot, C.J., Medvedev, S., Alavi, M., Shahrivar, H. & Heidari, E. 2000. Salt extrusion rates at Kuh-e-Jahani, Iran: June 1994 to November 1997. *In:* Vendeville, B.C., Mart, Y. & Vignerrese, J.L. (eds) *Salt, Shale and Igneous Diapirs in and around Europe*. Geological Society, London, Special Publications, **174**, 93–110.

Thorel, L. & Ghoreychi, M. 1996. Rock salt damage—experimental results and interpretation. *In:* Ghoreychi, M., Berest, P., Hardy, H.F., Jr & Langer, M. (eds) *The Mechanical Behaviour of Salt. Proceedings of the Third Conference, Palaiseau, France*. Trans Tech Publications, Clausthal, Switzerland, 175–189.

Wu, S., Bally, A.W. & Cramez, C. 1990. Allochthonous salt, structure, and stratigraphy of the north-eastern Gulf of Mexico. Part II, structure. *Marine and Petroleum Geology*, **7**, 334–370.

Zentilli, M., Kettanah, Y., Negulic, E., Wilens, H., Grist, A.M. & Brown, E.T. 2008. Thermal effects of salt on the petroleum system: evidence from fission track thermochronology, fluid inclusions and basin modelling. *In: Conjugate Margins Conference Halifax, University of Dalhousie, Halifax, Nova Scotia, Extended Abstracts* (CD ROM), 75–82.

Zirngast, M. 1996. The development of the Gorleben salt dome (northwest Germany) based on quantitative analysis of peripheral sinks. *In:* Alsop, G.I., Blundell, D. & Davison, I. (eds) *Salt Tectonics*. Geological Society, London, Special Publications, **100**, 203–226.

Received 27 May 2008; revised typescript accepted 13 October 2008.
Scientific editing by Ian Alsop.